Article

Discovery Medicine 2026; 38(212): 2960–2974
https://doi.org/10.24976/Discov.Med.202638212.228

Quantitative Features of Neovascularization in Fibrotic Age-Related Macular Degeneration and Their Associations With Visual Changes After a Single Anti-VEGF Therapy

Xinyue Zhu[1,2,3,†], Xincan Huang[1,†], Yuanyuan Gong[1,2,3], Huixun Jia[1,2,3], Yanlin Qu[1,2,3], Ting Shen[1,2,3], Jieqiong Chen[1,2,3], Minwen Zhou[1,2,3], Qiyu Bo[1,2,3,*], Ying Hu[1,2,3,*]

[1]Department of Ophthalmology, Shanghai General Hospital, Shanghai Jiao Tong University School of Medicine, 200080 Shanghai, China
[2]National Clinical Research Center for Eye Diseases, 200080 Shanghai, China
[3]Shanghai Key Laboratory of Ocular Fundus Diseases, 200080 Shanghai, China
*Correspondence: bonnieboqiyu@163.com (Qiyu Bo); dr_huying@163.com (Ying Hu)
[†]These authors contributed equally.
Submitted: 13 July 2026 Revised: 10 August 2026 Accepted: 25 August 2026 Published: 23 September 2026

Background: Macular fibrosis represents an advanced manifestation of neovascular age-related macular degeneration (nAMD), but active neovascularization may persist within fibrotic lesions. Reliable biomarkers for predicting short-term visual changes after anti-vascular endothelial growth factor (VEGF) therapy in eyes with fibrotic lesions remain limited. This study aimed to identify predictors associated with short-term visual changes 4 weeks after a single anti-VEGF therapy in patients with macular fibrosis (MF).

Methods: Patients with active nAMD, either treatment-naïve or without anti-VEGF therapy for ≥6 months, were included and classified into fibrotic and non-fibrotic groups. Within the MF cohort, associations between baseline clinical, optical coherence tomography (OCT), and optical coherence tomography angiography (OCTA) parameters and continuous changes in best-corrected visual acuity (BCVA) after a single injection were initially explored. Subsequently, patients were further divided into vision-improved (ΔBCVA ≥5 letters) and vision-unimproved (ΔBCVA <5 letters) groups after a single injection. Baseline clinical and OCTA parameters were compared. Quantitative vascular features were explored using logistic regression analysis.

Results: Seventy-five patients were included (48 with MF, 27 without). Within the fibrotic cohort, macular neovascularization (MNV) lesions showed a larger vessel area, greater vessel length, more endpoints, greater central macular thickness, and worse baseline BCVA. However, these differences cannot be fully separated from the potential effects of previous treatment exposure, as fibrosis status was completely confounded with treatment history in this cohort. After adjustment for lesion area, the differences in absolute vascular parameters, including vessel area, total vessel length, and endpoint, were no longer statistically significant. In addition, fibrotic lesions exhibited significant quantitative vascular changes after anti-VEGF therapy, characterized by reductions in total vessel length, endpoint count, and exudation, accompanied by an increase in lacunarity ($p < 0.001$). Within the MF cohort, the vision-improved group was younger ($p = 0.039$) and had higher baseline junction density ($p = 0.002$) compared with the vision-unimproved group. Receiver operating characteristic (ROC) analysis showed that the combination of age and junction density predicted short-term visual improvement with good accuracy (area under the curve (AUC) = 0.77, 95% CI: 0.64–0.91). Junction density alone was also predictive (AUC = 0.77, 95% CI: 0.62–0.93).

Conclusion: OCTA revealed that fibrotic MNV exhibited measurable vascular responsiveness after a single anti-VEGF therapy, as evidenced by significant post-treatment reductions in total vessel length, endpoint count, and exudation, together with an increase in lacunarity. More importantly, quantitative OCTA parameters, particularly junction density, predicted 4-week visual improvement with acceptable accuracy. These findings suggest that quantitative OCTA parameters may serve as candidate biomarkers of short-term visual change after a single anti-VEGF injection in patients with fibrotic nAMD.

Keywords: age-related macular degeneration; macular fibrosis; optical coherence tomography angiography; junction density; visual change

Introduction

Macular fibrosis has long been regarded as a hallmark of late-stage neovascular age-related macular degeneration (nAMD), typically indicating a relatively stable disease stage [1]. However, active neovascularization inside the scar challenges the historical notion of post-scarring stability. Longitudinal studies have demonstrated ongoing disease activity in fibrotic lesions, which often leads to progressive visual decline [2,3,4]. Preserving residual visual function constitutes a critical objective in the disease management of late nAMD. Despite this clinical need, our understanding of intra-fibrotic neovascularization remains limited, and reliable biomarkers associated with short-term visual changes after a single anti-vascular endothelial growth factor (VEGF) therapy in these patients are still lacking.

Fibrotic lesions typically appear as well-demarcated and elevated mounds of yellowish-white tissue on fundoscopy [4,5]; however, their internal architecture on optical coherence tomography (OCT) is highly heterogeneous. OCT has been shown to identify structural features associated with best-corrected visual acuity (BCVA)—for example, lesions with an intact retinal pigment epithelium (RPE) layer ('type-A') have better visual outcomes [6]. In addition, OCT structural features, for example, subretinal fluid (SRF) and intraretinal fluid (IRF), are clinically relevant and have been linked to visual function and disease activity [7]. However, whether these parameters can predict visual improvement following a single anti-VEGF therapy in eyes with advanced fibrotic nAMD lesions remains unclear, as fluid resolution does not always translate into visual gain. In addition, several optical coherence tomography angiography (OCTA)-derived vascular parameters (vessel area, junction density, vessel length, endpoint count, and lacunarity) have been shown to reflect lesion activity and sensitivity to anti-VEGF therapy [8,9]. Their predictive value for short-term treatment response—especially visual improvement—in fibrotic lesions remains unknown [8,9]. This uncertainty limits the ability to personalize anti-VEGF therapy in patients with fibrotic nAMD.

To address these gaps, we first compared the quantitative vascular differences of macular neovascularization (MNV) between fibrotic and non-fibrotic nAMD lesions, as well as their overall response following a single anti-VEGF therapy. Within the fibrotic cohort, we then analyzed differences in OCT-derived structural features (RPE continuity and the presence of SRF, IRF, or subretinal hyperreflective material (SHRM)) and OCTA-derived vascular parameters (vessel area, junction density, endpoint count, and lacunarity) between eyes with different visual outcomes. Finally, we explored key predictors of visual improvement and evaluated their predictive performance using receiver operating characteristic (ROC) analysis, aiming to explore imaging factors associated with short-term visual improvement after a single anti-VEGF therapy in patients with fibrotic nAMD.

Methods

Participants

This study was a retrospective exploratory cohort study. Patients with active nAMD, with or without macular fibrosis (MF), who received a single anti-VEGF therapy and were followed up at 4 weeks using OCT and OCTA at Shanghai General Hospital, Shanghai, China, from April 2019 to March 2022 were included. The research team systematically collected and organized clinical and imaging data of these patients in May 2026 for retrospective analysis. This study was approved by the Medical Ethics Committee of Shanghai General Hospital and conducted in accordance with the tenets of the Declaration of Helsinki. The requirement for written informed consent was waived by the Medical Ethics Committee because of the retrospective nature of the study. All analyzed data were anonymized and de-identified.

Eligible patients were either treatment-naïve or had not received anti-VEGF therapy for at least 6 months before the index injection. All fibrotic eyes included in this study had received previous anti-VEGF therapy, whereas all non-fibrotic eyes were treatment-naïve. This retrospective study included patients who had not received anti-VEGF therapy for at least six months before the index anti-VEGF injection. Baseline ophthalmic examination data, including BCVA, color fundus photography, OCT, and OCTA findings, as well as corresponding follow-up data at 4 weeks after a single intravitreal anti-VEGF therapy, were retrospectively collected from the medical records.

In this study, all non-fibrotic eyes received the same anti-VEGF therapy, 2 mg aflibercept (Eylea®, 2.0 mg/0.05 mL; Bayer AG, Berlin, Germany) [10]. Among the fibrotic group, 20 eyes were treated with 2 mg aflibercept, while the remaining 28 eyes received 4 mg efdamrofusp alfa (Code: IBI302, which targets both VEGF and complement components C3b/C4b) [11]. To evaluate whether the use of different agents within the fibrotic subgroup confounded the short-term treatment outcomes, we performed a prespecified subgroup analysis. In this analysis, we compared the pre-to-post treatment changes in OCTA-derived vascular parameters, BCVA, and visual outcomes between the aflibercept- and IBI302-treated eyes within the fibrosis group. The results of the subgroup analysis are summarized in **Supplementary Table 1**. No statistically significant differences were observed between the aflibercept and IBI302 groups for any of the assessed variables (all $p > 0.05$). However, given the limited sample size and the different pharmacological mechanisms of these two agents, the possibility of treatment-related heterogeneity cannot be completely excluded. Therefore, the findings should be interpreted with caution when pooling these treatment sub-

groups in subsequent analyses. The following inclusion criteria for this study were applied by 2 experienced ophthalmologists: (1) age >50 years; (2) exudative nAMD with or without MF; (3) lesion size <12 optic disc diameters; (4) fovea thickness >250 μm; (5) availability of pre- and post-treatment data on BCVA, CFP, OCT and OCTA; and (6) no treatment of the studied eye with anti-VEGF therapy, anti-complement drug therapy, laser photocoagulation therapy, photodynamic therapy, intraocular surgery, or glucocorticoid injection therapy within the preceding 6 months. The exclusion criteria were as follows: (1) MNV caused by conditions other than nAMD; (2) coexisting eye diseases, such as diabetic maculopathy, glaucoma and a history of retinal detachment; (3) systemic disease; or (4) poor image quality due to severe media opacity.

Grouping

The participants were classified into fibrotic and non-fibrotic groups on the basis of CFP and OCT. On CFP examination, a fibrotic lesion was defined as a well-demarcated, elevated mound of yellowish–white tissue [12]. On OCT, a lesion was defined as fibrotic if >50% of its area was occupied by compact, sheet-like hyperreflective material situated either above or beneath the RPE [13].

Two ophthalmologists independently classified the lesions on the basis of CFP, OCT and OCTA findings. A retina specialist adjudicated discrepancies. On this basis, to further evaluate short-term visual changes after anti-VEGF therapy, patients in the MF group were further stratified into the vision-improved and vision-unimproved groups according to changes in BCVA. Because visual acuity changes after a single anti-VEGF therapy are often modest, BCVA was evaluated using the Early Treatment Diabetic Retinopathy Study (ETDRS) letter score. Compared with conventional Snellen visual acuity charts, ETDRS letter scoring provides greater sensitivity and precision for detecting small changes in visual function and is therefore more suitable for assessing short-term treatment responses in patients with nAMD. Vision improvement was defined as an increase of ≥5 letters in BCVA after treatment, whereas vision unimproved was defined as an improvement of <5 letters or no improvement in BCVA following treatment. This threshold was selected based on previous studies of anti-VEGF therapy in nAMD, in which a change of approximately 5 ETDRS letters has been used to define a clinically meaningful change in visual acuity [14,15,16].

Clinical Examination

Data on the characteristics and examination findings of all included patients, including sex, age, BCVA, CFP (Visucam 200 Digital Fundus Camera; Carl Zeiss Meditec AG, Jena, Germany), OCT (Spectralis; Heidelberg Engineering GmbH, Heidelberg, Germany), and OCTA (PLEX Elite 9000; Carl Zeiss Meditec, Inc., Dublin, CA, USA), at baseline and at the 4-week's visit after a single anti-VEGF therapy were retrieved from medical records.

OCT Parameters

The following OCT parameters were analyzed: central macular thickness (CMT), macular choroidal thickness (MCT), presence of SRF, IRF, subretinal hyperreflective material (SHRM), and RPE continuity. CMT was automatically obtained from the Spectralis OCT system using the built-in retinal thickness analysis software and was defined as the retinal thickness within the central 1-mm ETDRS subfield, measured from the internal limiting membrane to Bruch's membrane–RPE complex. MCT was measured using the subfoveal choroidal thickness method. The measurement was defined as the vertical distance between the outer border of the RPE–Bruch's membrane complex and the choroid–scleral interface at the foveal center. Automated segmentation lines were manually corrected when necessary to ensure accurate delineation of the choroidal boundaries. Each measurement was performed three times, and the mean value was used for analysis.

Based on previous spectral-domain OCT classification systems for fibrotic lesions in neovascular AMD, a continuous RPE was defined as an intact, uninterrupted hyperreflective band corresponding to the retinal pigment epithelium layer on cross-sectional B-scans. Specifically, the RPE was considered continuous when it could be clearly identified without significant disruption, fragmentation, or loss of reflectivity throughout the fibrotic lesion and the surrounding macular area. This definition aligns with the morphological characteristics of Type A fibrotic lesions, in which the RPE remains mainly intact and preserved beneath the fibrotic material. In contrast, continuous RPE was absent in Type B lesions, where the RPE was disrupted or located within the lesion, and in Type C lesions, where the RPE was not discernible. Continuity of the RPE has been associated with better visual outcomes and fewer degenerative changes. All OCT assessments were independently performed by two masked investigators, who were blinded to clinical information and treatment outcomes. Any discrepancies between the two investigators were reviewed and resolved by a senior investigator.

SS-OCTA Image Acquisition and Quantitative Analysis

SS-OCTA images were acquired using the PLEX Elite 9000 system (Carl Zeiss Meditec, Inc., Dublin, CA, USA) with a 6 mm × 6 mm scan protocol, as previously described [17]. Image quality was assessed using the signal strength index (SSI), and images with an SSI <7 or significant motion artifacts were excluded from quantitative analysis [18]. This threshold was selected according to the manufacturer's recommended image quality criteria and was consistently applied to all scans. OCTA images were considered eligible for quantitative analysis when they showed adequate signal strength, clear visualization of the MNV lesion, and no significant motion artifacts or segmentation errors. Images with severe shadowing artifacts, incomplete lesion vi-

sualization, or uncorrectable segmentation errors were excluded. For en face imaging and quantitative analysis, the RPE-fit boundary layer provided by the PLEX Elite 9000 was used as the initial segmentation reference. The upper and lower boundaries of the segmentation slab were predefined by the RPE and RPE-fit reference line, respectively. The segmentation boundaries were manually adjusted on corresponding B-scans in each case to ensure complete inclusion of the MNV lesion, including areas associated with subretinal hyperreflective material or pigment epithelial detachment, while minimizing contamination from superficial retinal vessels. The integrated projection artifact removal function was used to eliminate artifacts originating from the retinal vasculature. Lesion borders were delineated from the background using Photoshop software (version 22.0; Adobe Inc., San Jose, CA, USA), and pixel measurements were converted to millimeters using the following equation: length (mm) = length(px) × 6/1024.

AngioTool software (version 0.6a; National Cancer Institute, Bethesda, MD, USA) was subsequently used to quantify the morphological and spatial characteristics of the MNV lesions (Fig. 1). According to previous studies using AngioTool for OCTA-based vascular analysis, the parameters for vessel detection and skeletonization can be optimized individually for each image to achieve accurate vessel delineation [8,19]. In the present study, the analysis parameters were adjusted according to the vascular visualization quality of each OCTA image. The vessel diameter parameter was set to 4, 5, or 6, and the vessel intensity threshold was adjusted within the range of 15–30. The "remove small particles" parameter was set to 100, while the "fill holes" function was not applied. For each eye, identical AngioTool parameters were applied to the baseline and 4-week OCTA images to ensure consistency in longitudinal comparisons. For output visualization, "Show overlay" was selected; the width settings for "Show outline", "Show skeleton", "Show branching points", and "Show boundary" were set to 1, 2, 4, and 1, respectively. The generated skeletonized images were visually compared with the corresponding en face OCTA images, and manual corrections were performed only for segmentation errors or artifacts when necessary [8,9]. Six vascular parameters, including vessel area, junction density, total vessel length, mean vessel length, number of endpoints, and average lacunarity, were calculated.

Junction density was calculated as the number of vascular junctions divided by the total vessel length and was originally generated by AngioTool with the unit of junctions/mm. To facilitate data presentation and statistical analysis, the raw junction density values were multiplied by 10,000. This linear transformation was uniformly applied to all samples and did not alter the relative differences among groups.

Two masked investigators, who were blinded to clinical information and treatment outcomes, independently performed OCTA image processing and quantitative analysis. Any discrepancies between the two investigators regarding image segmentation, parameter selection, or quantitative measurements were discussed and reviewed based on the corresponding OCTA images. Any discrepancies between the two investigators were reviewed and resolved by a senior investigator.

Statistical Analysis

Statistical analyses were performed using IBM SPSS Statistics version 26.0 (IBM Corp., Armonk, NY, USA). Continuous variables are presented as median (interquartile range, IQR), and categorical variables are presented as number and percentage [n (%)]. The normality of all data was assessed using the Kolmogorov–Smirnov test. The results indicated that none of the variables followed a normal distribution; therefore, nonparametric statistical methods were used for analysis. The Mann–Whitney U test was used to compare continuous variables between independent groups. The Wilcoxon signed-rank test was used to compare paired continuous variables before and after treatment. Spearman rank correlation analysis was performed to assess the associations between continuous baseline parameters and changes in BCVA after treatment. This nonparametric method was selected because the continuous variables did not follow a normal distribution and because Spearman correlation does not require a linear relationship between variables or normally distributed data, allowing the evaluation of monotonic relationships between variables. The Spearman correlation coefficient (r) was used to quantify the strength and direction of these associations. For categorical variables, the Pearson chi-square test or continuity-corrected chi-square test was used according to the expected cell counts. A p value < 0.05 (two-sided) was considered statistically significant.

Given the exploratory nature of this study, which aimed to identify potential imaging biomarkers associated with short-term visual changes after a single anti-VEGF therapy, no formal adjustment for multiple comparisons was performed. The analyses of OCT- and OCTA-derived parameters were considered hypothesis-generating, and the findings require further validation in larger prospective cohorts.

Variables that were statistically significant in univariate analysis were further evaluated using multivariable binary logistic regression analysis to identify independent predictors of short-term visual improvement. Age and junction density were entered as continuous variables in the logistic regression model. Odds ratios (ORs) and 95% confidence intervals (CIs) were calculated.

ROC curve analysis was subsequently performed for independent predictors identified in the multivariable analysis to determine their discriminative performance, including AUC, optimal cutoff value determined by the Youden index, sensitivity, and specificity. A combined predictive

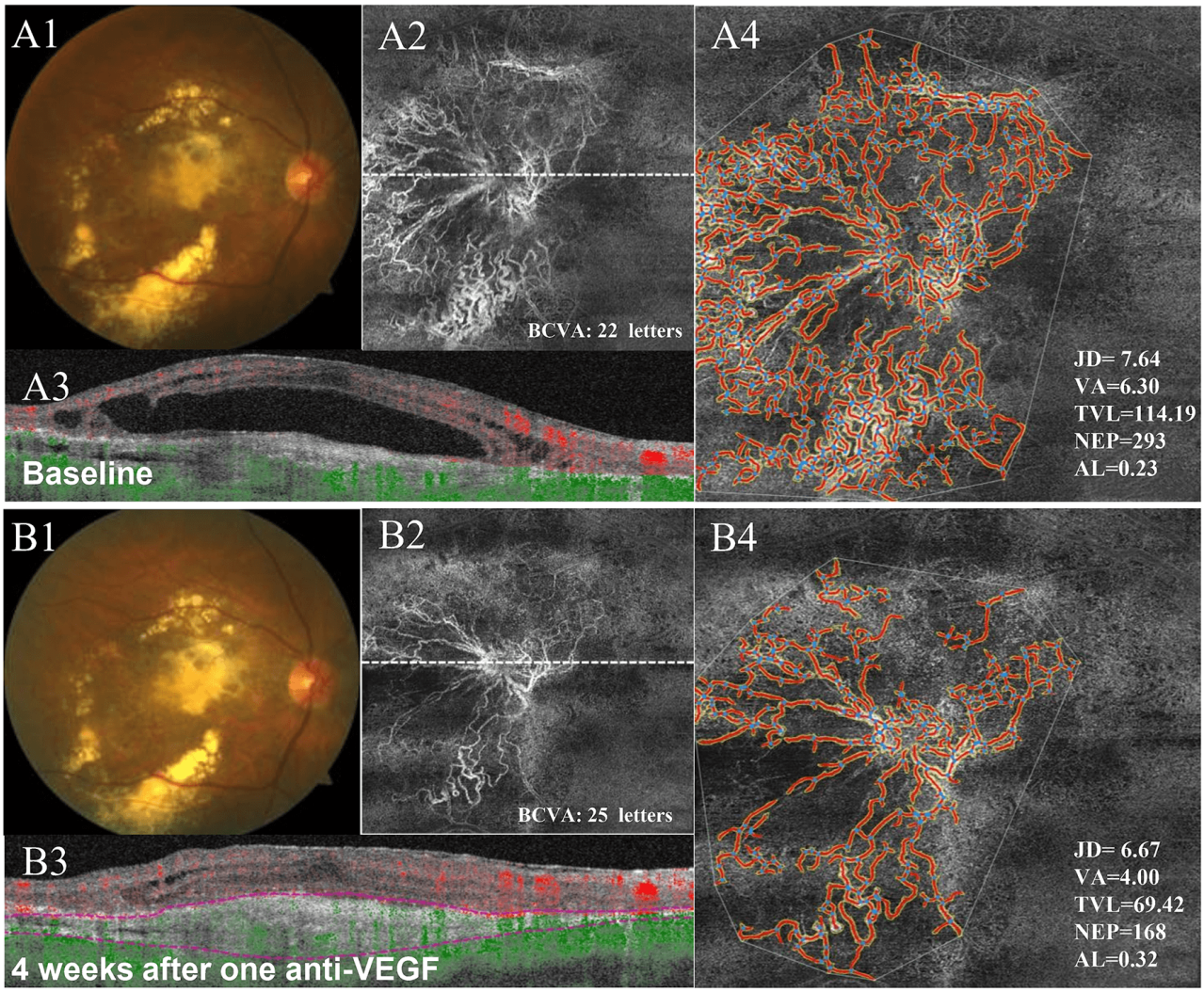

Fig. 1. Changes in OCTA and vascular parameters of fibrotic MNV before and after a single anti-VEGF therapy. (A1) Fundus of a fibrotic patient at the initial visit. (A2) En face OCTA image of a fibrotic patient at the initial visit. (A3) B-scan indicating a fibrotic lesion with SRF and IRF. (A4) Lesion reconstruction using AngioTool software: the vascular skeleton is shown in red and branching points in blue. JD, Junction Density; VA, Vessel Area; TVL, Total Vessel Length; NEP, Number of End Points; AL, Average Lacunarity. (B1) Fundus of fibrotic patient 4 weeks after a single anti-VEGF therapy. (B2) En face OCTA image represents regression of MNV 4 weeks after a single anti-VEGF therapy. (B3) B-scan indicating regression of SRF and IRF 4 weeks after a single anti-VEGF therapy. (B4) Lesion reconstruction using AngioTool software displayed regression of vascular parameters of fibrotic MNV. OCTA, optical coherence tomography angiography; MNV, macular neovascularization; VEGF, vascular endothelial growth factor; SRF, subretinal fluid; IRF, intraretinal fluid.

model incorporating age and junction density as continuous variables was subsequently constructed. The predictive performance of this combined model was evaluated using ROC analysis. ROC curve plotting and calculation of ROC-related parameters were performed using R software (version 4.5.2; R Foundation for Statistical Computing, Vienna, Austria).

Results

Demographics

Seventy-five eyes from 75 patients with nAMD were included in this study, including 48 eyes with MF (38 males and 10 females) and 27 eyes without fibrosis (18 males and 9 females). Among the fibrotic eyes, 17 eyes were classified into the vision-improved group (13 males and 4 females) and 31 eyes into the unimproved group (25 males and 6 females). The median age of participants was 69 (65, 73.5) years.

Table 1. Patient characteristics and quantitative analysis of MNV with or without MF among nAMD patients at baseline.

Baseline	Fibrotic nAMD (n = 48)	Non-fibrotic nAMD (n = 27)	Test statistic	*p*-value
Age (years)	69 (65, 73)	68 (65, 76)	Z = 0.326	0.744[a]
Sex, n(%)			χ^2 = 1.427	0.232[b]
Female	10 (20.83%)	9 (33.3%)		
Male	38 (79.17%)	18 (66.67%)		
Exudation	48 (100%)	27 (100%)		
CMT[1] (μm)	557 (366.75, 682.25)	402 (336, 554.25)	Z = 2.434	**0.015**[a*]
BCVA (ETDRS-Score)	31.5 (21, 42.75)	58 (45, 63)	Z = –5.043	**<0.001**[a*]
MNV lesion area (mm^2)	9.06 (6.21, 14.99)	3.62 (2.72, 5.54)	Z = 4.790	**<0.001**[a*]
Vessel area (mm^2)	2.77 (1.89, 4.46)	1.24 (0.72, 1.57)	Z = 4.901	**<0.001**[a*]
Junction density[2] (junctions/dm^2)	8.96 (6.10, 13.08)	11.20 (9.32, 13.59)	Z = –1.810	0.070[a]
Total vessel length (mm)	56.78 (36.50, 89.98)	24.91 (18.22, 36.63)	Z = 4.868	**<0.001**[a*]
Average vessel length (mm)	5.69 (3.03, 10.37)	5.58 (3.92, 13.51)	Z = –0.309	0.757[a]
Number of endpoints	151 (104.25, 245.5)	74 (51, 104)	Z = 4.349	**<0.001**[a*]
Average lacunarity	0.32 (0.25, 0.42)	0.34 (0.24, 0.46)	Z = –0.751	0.453[a]

[1]Central Macular Thickness, [2] Junction density values were multiplied by 10,000 from the original AngioTool output for statistical analysis and visualization.

Data are presented as median (IQR) for continuous variables and n (%) for categorical variables.

[a] Mann-Whitney U test; [b] Pearson chi-square test; Bold *p* values and those marked with an asterisk (*) indicate statistical significance ($p < 0.05$).

Vascular Differences Between MNVs With and Without a MF

Lesions were divided into two groups on the basis of the existence of MF: the fibrotic nAMD group (n = 48) and the non-fibrotic nAMD group (n = 27). There were no significant differences between the two groups in terms of age, sex, exudation, or OCTA parameters, including junction density ($p = 0.070$), average vessel length ($p = 0.757$), and average lacunarity ($p = 0.453$). The median BCVA of the fibrotic group at baseline was 31.5 (21, 42.75). The median BCVA of the non-fibrotic group before treatment was 58 (45, 63) ETDRS letter score ($p < 0.001$). The CMTs of both groups at baseline were 557 (366.75, 682.25) μm and 402 (336, 554.25) μm, respectively ($p = 0.015$). In addition, vessel area ($p < 0.001$), total vessel length ($p < 0.001$) and the number of endpoints ($p < 0.001$) were greater in the fibrotic group than in the non-fibrotic group. These results confirmed that MNV observed in fibrotic lesions was associated with poorer BCVA, a greater CMT, larger vessel area, and longer vessel length. However, because fibrosis status was completely confounded with previous treatment exposure in this cohort, these differences cannot be attributed solely to fibrosis. The baseline characteristics and quantitative analysis of the patients are presented in Table 1. Because vessel area, total vessel length, and number of endpoints are potentially influenced by MNV lesion size, additional multivariable linear regression analyses were performed after adjustment for MNV lesion area. After adjustment for MNV lesion area, the previously observed differences in vessel area, total vessel length, and the number of endpoints between fibrotic and non-fibrotic lesions were no longer statistically significant (**Supplementary Table 2**).

Vascular Parameters Changes of MNV With MF and Without MF After a Single Anti-VEGF Therapy

By analyzing the vascular characteristics of the participants before and after anti-VEGF therapy via OCTA, we observed significant changes in several quantitative vascular parameters within both the fibrotic and non-fibrotic groups. Specifically, vessel area, total vessel length, and number of endpoints decreased after treatment, whereas average lacunarity increased ($p < 0.05$). These findings indicate that MNV lesions in both groups exhibited measurable vascular alterations following anti-VEGF therapy. In addition, in the non-fibrotic group, the junction density and average vessel length were decreased by 18.12% (IQR, –9.37% to 37.03%, $p = 0.037$) and 37.55% (IQR, –34.49% to 66.85%, $p = 0.027$), respectively, compared with baseline values (Table 2).

Regression of exudation and CMT were used as indicators to evaluate short-term anatomical changes after anti-VEGF therapy. We found that some patients developed a dry macula or significantly reduced exudation after anti-VEGF therapy. The proportions of patients with resolution of exudation in the fibrotic and non-fibrotic groups at 4 weeks after injection were 41.67% and 70.37%, respectively. CMT significantly decreased by 31.36% (IQR, 14.47% to 45.75%, $p < 0.001$) and 26.42% (IQR, 21.19% to 55.06%, $p < 0.001$) in the fibrotic and non-fibrotic groups, respectively. Furthermore, BCVA was better in the non-fibrotic group than in the fibrotic group at baseline ($p < 0.001$). BCVA improved from 31.5 (21, 42.75) to 34.00 (23.25, 51.5) ETDRS letter score in the fibrotic group ($p < 0.001$), while improved from 58 (45, 63) to 66.00 (56.5, 73.5) ETDRS letter score in the non-fibrotic group after a

Table 2. Quantitative analysis of MNV before and after anti-VEGF therapy between two groups.

	Fibrotic nAMD (n = 48)					Non-fibrotic nAMD (n = 27)					VS.	
	Baseline	4 w	Decline rate (%)	Test statistic①	*p*-value①	Baseline	4 w	Decline rate (%)	Test statistic②	*p*-value②	Test statistic③	*p*-value③
Vessel area (mm^2)	2.77 (1.89, 4.46)	1.58 (0.98, 2.86)	33.33 (22.61, 51.56)	Z = –5.949	**<0.001**[a*]	1.24 (0.72, 1.57)	0.75 (0.48, 1.14)	34.04 (7.02, 46.86)	Z = –3.844	**<0.001**[a*]	Z = –0.629	0.529[b]
Junction Density[1] (junctions/dm^2)	8.96 (6.10, 13.08)	8.96 (6.19, 11.69)	13.94 (–24.81, 27.15)	Z = –1.323	0.186[a]	11.20 (9.32, 13.59)	9.30 (7.17, 12.80)	18.12 (–9.37, 37.03)	Z = –2.090	**0.037**[a*]	Z = –0.949	0.342[b]
Total vessel length (mm)	56.78 (36.50, 89.98)	35.97 (25, 60.37)	27.98 (14.92, 40.54)	Z = –5.846	**<0.001**[a*]	24.91 (18.22, 36.63)	17.61 (10.45, 22.15)	25.91 (12.66, 38.90)	Z = –3.508	**<0.001**[a*]	Z = –0.320	0.749[b]
Average vessel length (mm)	5.69 (3.03, 10.37)	5.04 (2.70, 9.03)	14.78 (–39.13, 55.99)	Z = –1.241	0.215[a]	5.58 (3.92, 13.51)	4.00 (2.47, 7.08)	37.55 (–34.49, 66.85)	Z = –2.210	**0.027**[a*]	Z = –1.004	0.315[b]
Number of endpoints	151 (104.25, 245.5)	123 (86.50, 205.5)	13.66 (–1.46, 30.68)	Z = –3.540	**<0.001**[a*]	74 (51, 104)	62 (42, 94)	19.05 (–14.89, 29.01)	Z = –2.128	**0.033**[a*]	Z = –0.320	0.749[b]
Average lacunarity	0.32 (0.25, 0.42)	0.42 (0.30, 0.55)	–31.70 (–50.56, –11.25)	Z = –4.985	**<0.001**[a*]	0.34 (0.24, 0.46)	0.40 (0.30, 0.56)	–25.51 (–54.29, -1.8)	Z = –3.267	**0.001**[a*]	Z = –0.210	0.834[b]
Exudation[2], n(%)	48 (100%)	28 (58.33%)	41.67	-	**<0.001**[d*]	27 (100%)	8 (29.63%)	70.37	-	**<0.001**[d*]	χ^2 = 5.704	**0.017**[c*]
CMT (μm)	557 (366.75, 682.25)	347 (276.5, 456)	31.36 (14.47, 45.75)	Z = –5.939	**<0.001**[a*]	402 (336, 554.25)	284 (221, 372)	26.42 (21.19, 55.06)	Z = –4.045	**<0.001**[a*]	Z = –0.706	0.480[b]
BCVA (ETDRS-Score)	31.5 (21, 42.75)	34.00 (23.25, 51.5)	–7.11 (–22.67, 1.42)	Z = –4.006	**<0.001**[a*]	58 (45, 63)	66.00 (56.5, 73.5)	–9.68 (–41.29, –4.40)	Z = –3.926	**<0.001**[a*]	Z = –1.628	0.104[b]

[1]Junction density values were multiplied by 10,000 from the original AngioTool output for statistical analysis and visualization.

[2]For exudation, a paired binomial test was used because all eyes had exudation at baseline. As this test provides exact *p* values directly from the binomial distribution, no test statistic is reported.

[a] Wilcoxon test; [b] Mann-Whitney U test; [c] Pearson chi-square test; [d] Paired binomial test; Bold *p* values and those marked with an asterisk (*) indicate statistical significance ($p < 0.05$).

① Test statistics and *p*-values represent within-group comparisons between baseline and 4 weeks in the Fibrotic nAMD group.

② Test statistics and *p*-values represent within-group comparisons between baseline and 4 weeks in the Non-fibrotic nAMD group.

③ Test statistics and *p*-values represent between-group comparisons between the Fibrotic nAMD and Non-fibrotic nAMD groups.

Data are presented as median (IQR) for continuous variables and n (%) for categorical variables. “Decline rate” refers to “4 weeks” vs “baseline”. (baseline-4 weeks)/baseline ×100%.

VS.: comparison of changes between the fibrotic and non-fibrotic groups.

Table 3. Associations between continuous variables and Change in BCVA 4 weeks after a single injection.

Variable	Spearman correlation coefficient (r)	*p*
Age	–0.316	**0.029***
CMT (μm)	–0.192	0.190
MCT[1] (um)	–0.020	0.891
Baseline BCVA	0.132	0.370
Vessel area (mm^2)	–0.260	0.075
Junction Density[2] (junctions/dm^2)	0.429	**0.002***
Total vessel length (mm)	–0.186	0.205
Average vessel length (mm)	0.017	0.910
Number of end points	–0.101	0.496
Average lacunarity	–0.225	0.125

[1] Macular Choroidal Thickness, [2] Junction density values were multiplied by 10,000 from the original AngioTool output for statistical analysis and visualization.

Data were analyzed using Spearman correlation analysis. r indicates the Spearman correlation coefficient. Bold *p* values and those marked with an asterisk (*) indicate statistical significance ($p < 0.05$).

single anti-VEGF therapy ($p < 0.001$). However, these differences were not significant between the two groups ($p > 0.05$). These results suggest that MNV lesions with and without MF both exhibited short-term changes in quantitative vascular parameters after a single anti-VEGF therapy, indicating that neovascular lesions within fibrotic areas retain treatment responsiveness. The quantitative results are presented in Table 2.

Associations Between Baseline Parameters and Changes in BCVA After a Single Injection in Patients With MF

Correlation analyses were performed to evaluate the associations between baseline parameters and changes in BCVA 4 weeks after a single injection. To avoid information loss caused by dichotomizing visual changes, ΔBCVA was initially analyzed as a continuous variable. Among continuous variables, age ($r = –0.316$, $p = 0.029$) and junction density ($r = 0.429$, $p = 0.002$) were significantly associated with ΔBCVA, whereas other continuous parameters showed no significant associations (all $p > 0.05$). No significant associations were observed between categorical variables, including SRF, IRF, continuous RPE structure, and SHRM, and ΔBCVA (all $p > 0.05$). The results of continuous and categorical variable correlation analyses are presented in Tables 3,4, respectively.

To further evaluate clinically meaningful visual improvement, we performed an exploratory categorical analysis using a predefined threshold of ΔBCVA ≥5 letters. Among the MF cohort, patients were stratified into the vision improved group (n = 17) and the vision unimproved group (n = 31) based on post-treatment visual changes after a single injection. Among the patients in the vision unimproved group, 12 eyes showed visual decline (ΔBCVA <0 letters) 4 weeks after injection. No significant differences

Table 4. Associations between categorical variables and Change in BCVA 4 weeks after a single injection.

Variable	ΔBCVA	Test statistic	*p*
Sex		Z = –0.115	0.909
Male (n = 38)	2.5 (–0.25, 6.25)		
Female (n = 10)	2.5 (–1, 9.5)		
Fluid, SRF[1]		Z = –1.055	0.291
Yes (n = 21)	3 (0, 8)		
No (n = 27)	0 (–1, 9)		
Fluid, IRF[2]		Z = –1.731	0.083
Yes (n = 42)	1 (–1, 6)		
No (n = 6)	11 (2.5, 17)		
Continuous RPE		Z = –1.819	0.069
Yes (n = 28)	4 (0, 10.75)		
No (n = 20)	0 (–1, 4.5)		
SHRM[3]		Z = –0.973	0.331
Yes (n = 15)	3 (1, 6)		
No (n = 33)	0 (–1, 9)		

[1] Subretinal fluid, [2] Intraretinal fluid, [3] Subretinal Hyperreflective Material.

Data are presented as median (IQR) for continuous variables. Mann-Whitney U test.

were observed between the two groups in terms of sex, baseline CMT, MCT, baseline BCVA, SRF, IRF, continuous RPE structure or subretinal hyperreflective material (SHRM) (all $p > 0.05$). Age differed significantly between the groups, with the vision-unimproved group being older ($p = 0.039$).

Regarding quantitative vascular parameters, junction density was significantly higher ($p = 0.002$) in the vision-improved group compared with the vision-unimproved group. No significant differences were observed between the groups regarding vessel area, total vessel length, aver-

Table 5. Characteristics for vision-improved MF lesions and vision-unimproved MF lesions.

	Vision-improved fibrotic nAMD (n = 17)	Vision-unimproved fibrotic nAMD (n = 31)	Test statistic	*p*
Age	68 (63, 73)	70 (67, 74)	Z = –2.066	**0.039**[a*]
Sex, n (%)			χ^2 = 0.000	1.000[b]
Female	4 (23.53%)	6 (19.35%)		
Male	13 (76.47%)	25 (80.66%)		
CMT (μm)	485.00 (385.5, 610.50)	595 (359, 770)	Z = –1.229	0.219[a]
MCT[1] (um)	277 (218, 330)	270 (211, 357)	Z = –0.313	0.755[a]
Baseline BCVA	32 (14.5, 48.5)	31 (21, 42)	Z = –0.227	0.821[a]
Fluid, SRF[2], n (%)			χ^2 = 0.904	0.342[c]
Yes	9 (52.94%)	12 (38.71%)		
No	8 (47.06%)	19 (61.29%)		
Fluid, IRF[3], n (%)			χ^2 = 1.574	0.210[b]
Yes	13 (76.47%)	29 (93.55%)		
No	4 (23.53%)	2 (6.45%)		
Continuous RPE, n (%)			χ^2 = 1.626	0.202[c]
Yes	12 (70.59%)	16 (51.61%)		
No	5 (29.41%)	15 (48.39%)		
SHRM[4], n (%)			χ^2 = 0.041	0.839[c]
Yes	5 (29.41%)	10 (32.26%)		
No	12 (70.59%)	21 (67.74%)		
Vessel area (mm^2)	2.26 (1.24, 3.93)	3.36 (1.97, 4.52)	Z = –1.347	0.178[a]
Junction density[5] (junctions/dm^2)	13.22 (9.74, 15.12)	8 (5.75, 9.78)	Z = –3.115	**0.002**[a*]
Total vessel length (mm)	52.16 (31.25, 68.67)	70.38 (36.87, 95.48)	Z = –1.046	0.296[a]
Average vessel length(mm)	7.37 (3.28, 22.81)	5.10 (2.88, 8.88)	Z = –1.369	0.171[a]
Number of endpoints	147 (79, 208)	159 (108, 276)	Z = –1.046	0.296[a]
Average lacunarity	0.26 (0.21, 0.41)	0.33 (0.27, 0.42)	Z = –1.628	0.104[a]
Change in BCVA	10 (6.5, 17)	0 (–1, 2)	Z = –5.712	<0.001[a*]

[1] Macular Choroidal Thickness, [2] Subretinal fluid, [3] Intraretinal fluid, [4] Subretinal Hyperreflective Material, [5] Junction density values were multiplied by 10,000 from the original AngioTool output for statistical analysis and visualization.

Data are presented as median (IQR) for continuous variables and n (%) for categorical variables.

[a] Mann-Whitney U test; [b] Continuity-corrected chi-square test; [c] Pearson chi-square test; Bold *p* values and those marked with an asterisk (*) indicate statistical significance ($p < 0.05$).

age vessel length, number of vessel endpoints, or average lacunarity (all $p > 0.05$). Details are presented in Table 5.

The findings from this categorical analysis were consistent with those obtained from the continuous ΔBCVA analysis, with older age associated with less improvement and higher junction density associated with greater improvement.

Therefore, the categorical definition of visual improvement (ΔBCVA ≥5 letters) was subsequently used for multivariable logistic regression and ROC curve analyses to explore potential predictors of clinically meaningful visual improvement.

Multivariable Predictive Model and ROC Analysis

In the multivariable analysis including age and junction density, both variables remained statistically significant ($p < 0.05$) and were identified as independent predictors of visual improvement. Age was negatively associated with visual improvement (OR = 0.847, 95% CI: 0.730–0.983, $p = 0.029$), while junction density was positively associated with visual improvement (OR = 1.165, 95% CI: 1.007–1.348, $p = 0.039$). Details are presented in Table 6.

Table 6. Multivariable Logistic Regression Analysis for vision-improved MF lesions and vision-unimproved MF lesions.

	OR (95% CI)	*p*
Age	0.847 (0.730, 0.983)	**0.029***
Junction density	1.165 (1.007, 1.348)	**0.039***

Data are presented as odds ratio (OR) and 95% confidence interval (CI). Binary logistic regression analysis (multivariable); Bold *p* values and those marked with an asterisk (*) indicate statistical significance ($p < 0.05$).

ROC curve analysis identified an optimal baseline junction density cutoff of 10.56 for predicting visual improvement (Youden index = 0.57), yielding a sensitivity of

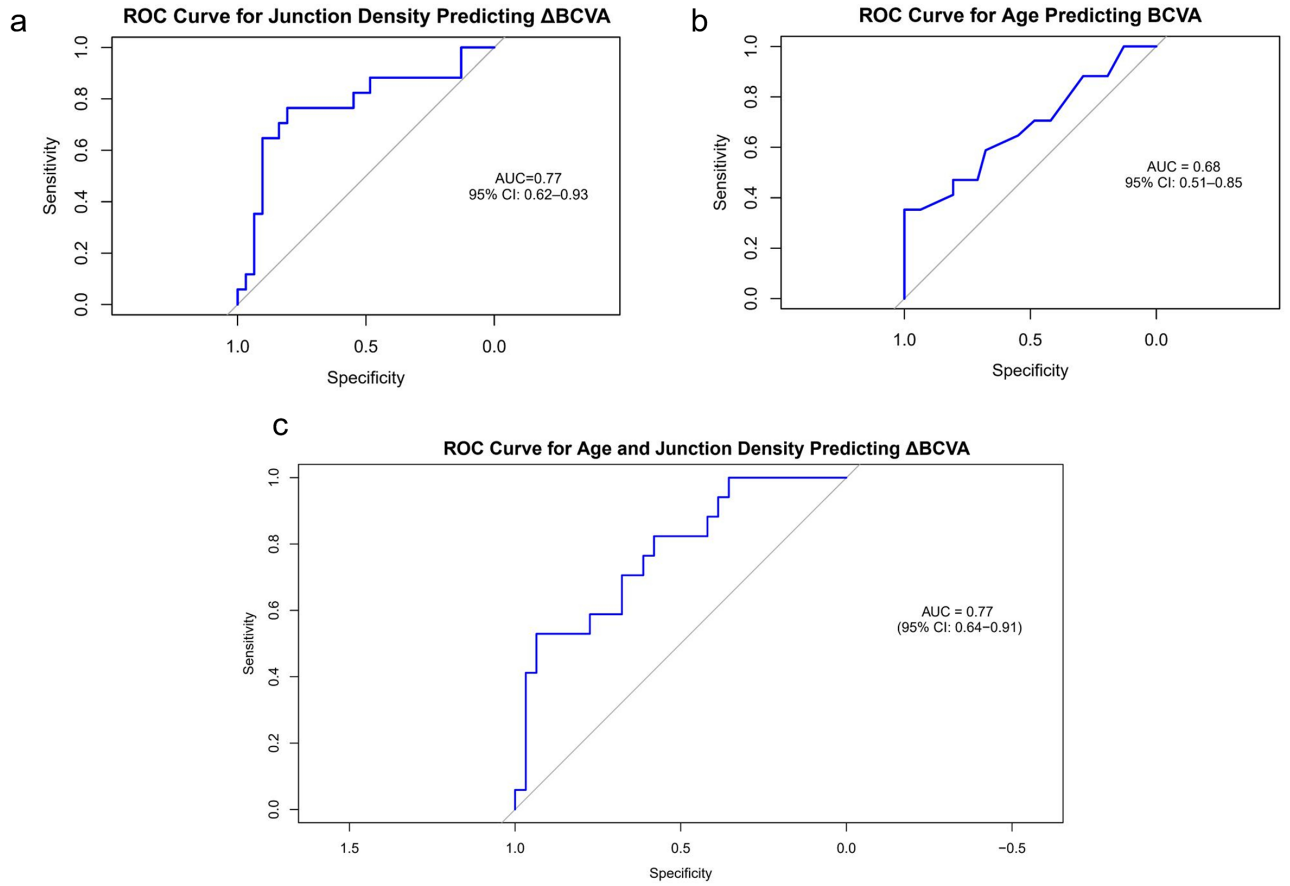

Fig. 2. ROC curves of junction density, age, and their combination for predicting short-term visual improvement (ΔBCVA ≥5 letters) after a single anti-VEGF therapy in fibrotic nAMD. (a) ROC curve of junction density for predicting short-term visual improvement (ΔBCVA ≥5 letters) after a single anti-VEGF therapy in fibrotic nAMD. (b) ROC curve of age for predicting short-term visual improvement (ΔBCVA ≥5 letters) after a single anti-VEGF therapy in fibrotic nAMD. (c) ROC curve of age and junction density for predicting short-term visual improvement (ΔBCVA ≥5 letters) after a single anti-VEGF therapy in fibrotic nAMD.

76.5% and a specificity of 80.6% (AUC = 0.77, 95% CI: 0.62–0.93) (Fig. 2a).

ROC curve analysis identified an optimal age cutoff of 63.5 for predicting visual improvement (Youden index = 0.35), yielding a sensitivity of 35.3% and a specificity of 100% (AUC = 0.68, 95% CI: 0.51–0.85) (Fig. 2b).

The final multivariable logistic regression model incorporated age and junction density as continuous variables. This model demonstrated an AUC of 0.77 (95% CI: 0.64–0.91) for predicting short-term visual improvement, with a sensitivity of 52.9% and a specificity of 93.5% (Fig. 2c).

To assess the robustness of the predictive model and quantify potential optimism due to the limited sample size, internal validation was performed using 1000 bootstrap resamples. In each bootstrap iteration, the logistic regression model was refitted using the prespecified predictors (age and junction density), and model performance was evaluated in both the bootstrap sample and the original dataset to estimate optimism. After optimism correction, the model demonstrated an AUC of 0.72 (95% CI: 0.61–0.82). Calibration assessment showed an optimism-corrected calibration slope of 0.67 and a Brier score of 0.17 (Fig. 3 and **Supplementary Table 3**), indicating moderate calibration performance after internal validation. These findings suggest that the combined model retains potential predictive utility for short-term visual improvement following anti-VEGF therapy in patients with fibrotic lesions.

In an exploratory analysis, junction density was dichotomized according to the Youden index-derived cutoff value of 10.56, and an additional logistic regression model incorporating age as a continuous variable and junction density as a dichotomized variable (high vs. low junction density) was evaluated. This exploratory model demonstrated an apparent AUC of 0.87 (95% CI: 0.76–0.98), with a sensitivity of 82.4% and a specificity of 87.1%. However, this cutoff value was derived from the same cohort and may introduce optimism bias due to data-driven threshold optimization. Therefore, the cutoff value of 10.56 was considered an exploratory parameter rather than a clinical thresh-

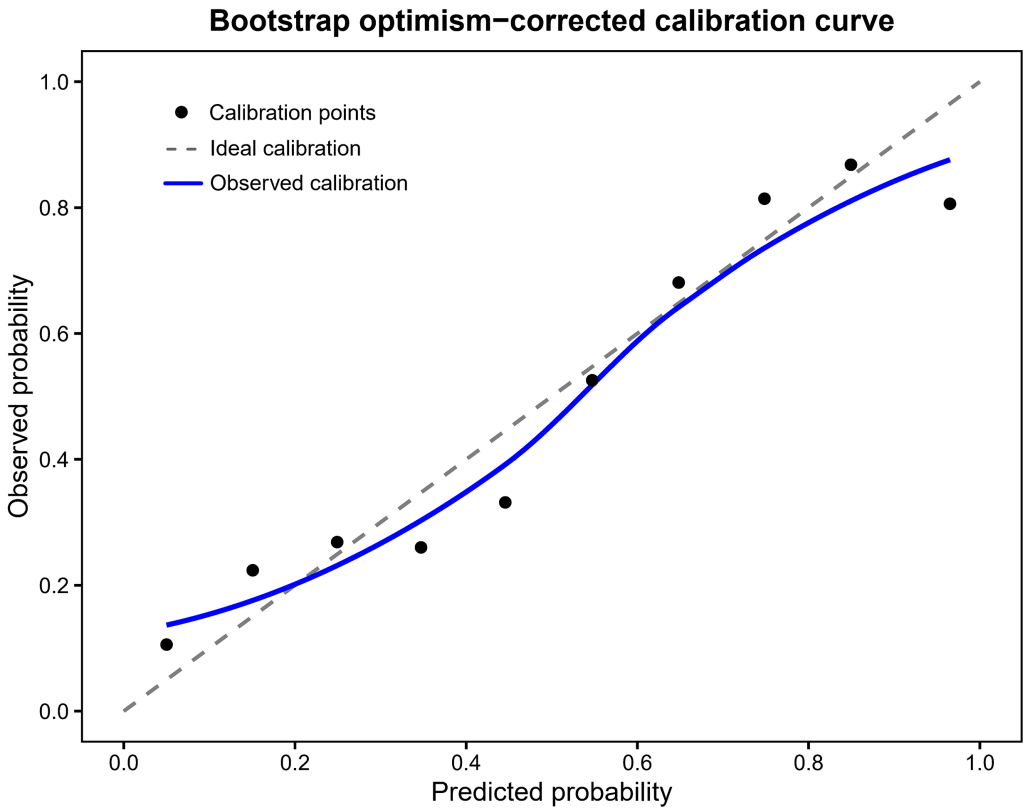

Fig. 3. Calibration curve of the internally validated prediction model. Calibration performance of the multivariable logistic regression model incorporating age and junction density was evaluated. The x-axis represents the predicted probability of visual improvement (ΔBCVA ≥5 letters), and the y-axis represents the observed proportion of patients with visual improvement. The gray dashed line indicates ideal calibration, and the blue solid line represents the observed calibration curve. The calibration curve showed reasonable agreement with the ideal reference line.

old. The results of this exploratory analysis are provided in **Supplementary Fig. 1** and **Supplementary Table 4**.

Distribution of Junction Density in Fibrotic and Non-Fibrotic Cohorts and Its Relationship With Visual Improvement

To visually illustrate the distribution of baseline vascular parameters across different cohorts and the association between junction density and visual improvement within the MF group, an ellipse-scatter plot was generated, with baseline junction density on the x-axis and ΔBCVA on the y-axis. Fibrotic and non-fibrotic patients were represented by circles in different colors, while within the MF cohort, red dots indicated patients with visual improvement and blue dots indicated patients without visual improvement.

This scatter plot visually demonstrates that: (1) Non-fibrotic lesions exhibited higher baseline junction density than fibrotic lesions, although the difference did not reach statistical significance, possibly due to the limited sample size (p = 0.07); (2) among fibrotic eyes, those with visual improvement (red dots) were clustered at higher baseline junction density, whereas eyes without improvement (blue dots) showed lower baseline junction density; and (3) a baseline junction density above a certain threshold (≥10.56) may be associated with short-term visual improvement after a single anti-VEGF therapy, even in the presence of established fibrosis, suggesting that junction density could serve as an imaging biomarker associated with short-term visual improvement after injection (Fig. 4).

Discussion

In this study, we found that MNV within fibrotic lesions exhibited measurable vascular responsiveness after a single anti-VEGF therapy, as evidenced by significant post-treatment reductions in total vessel length, endpoint count, and exudation, accompanied by increased lacunarity (all p < 0.001). These findings indicate that neovascularization within fibrotic lesions remains targetable despite the presence of fibrosis. Within the fibrotic cohort, younger age and higher baseline junction density each independently predicted short-term visual improvement. ROC analysis showed that the combination of age and junction density predicted 4-week visual improvement with acceptable accuracy (AUC = 0.77, 95% CI 0.64–0.91). Notably, junc-

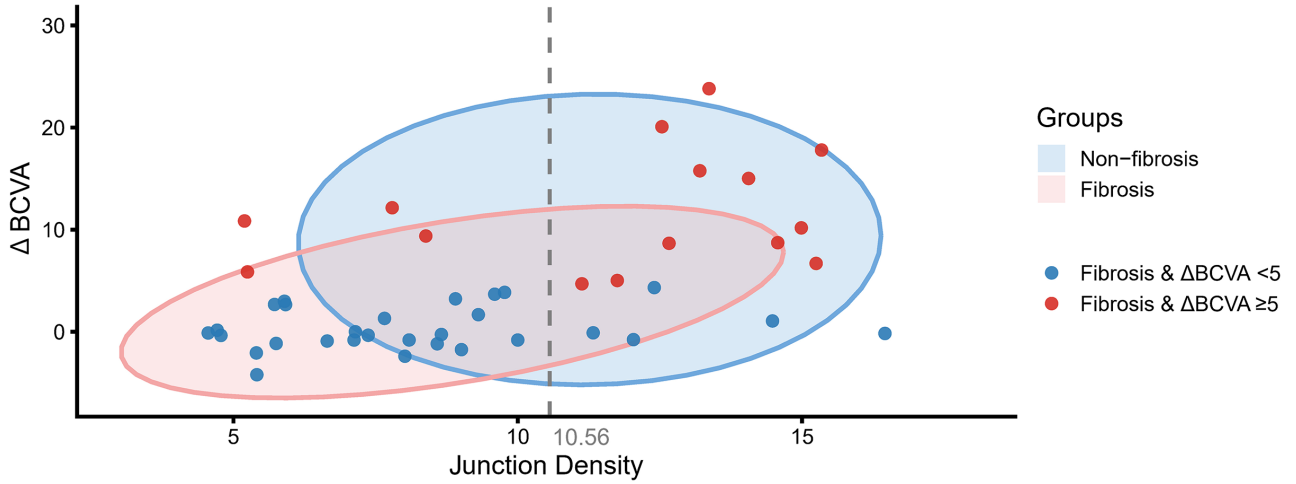

Fig. 4. The ellipses represent the distribution of junction density in fibrotic and non-fibrotic cohorts. The red and blue scatter points indicate the differences in junction density distribution between vision-improved and vision-unimproved patients within the fibrotic group.

tion density alone showed comparable performance (AUC = 0.77, 95% CI 0.62–0.93), suggesting that age provides limited incremental value beyond vascular connectivity. These findings support quantitative OCTA parameters—particularly junction density—as candidate biomarkers of short-term visual change after a single anti-VEGF injection in fibrotic nAMD.

MF represents the most common natural sequela of MNV and usually indicates the late stage of AMD [5,20]. In our cohort, baseline structural OCT characteristics were not significantly associated with short-term visual improvement, whereas OCTA revealed that fibrotic MNV lesions had larger vessel area, greater total vessel length, more endpoints, greater central macular thickness, and worse baseline BCVA than non-fibrotic lesions, which is consistent with the findings of Roberts et al. [21]. These observations should be interpreted cautiously because previous anti-VEGF exposure was completely confounded with fibrosis status. Furthermore, after adjustment for lesion area, the differences in absolute vascular measurements, including vessel area, total vessel length, and endpoint count, were no longer statistically significant, suggesting that these larger absolute vascular parameters may primarily reflect larger lesion size rather than increased intrinsic vascular complexity. Among fibrotic MNV lesions, 17/48 eyes achieved clinically meaningful visual improvement (ΔBCVA ≥5 letters) after a single anti-VEGF therapy, with a median BCVA gain of 10 letters (IQR, 6.5–17). These findings indicate that some fibrotic lesions may still exhibit short-term anatomical and functional changes after a single anti-VEGF therapy, although the long-term therapeutic implications require further investigation.

A previous study has suggested that quantitative OCTA-derived vascular features may provide information on the biological characteristics and treatment response of neovascular lesions [22]. In the present study, although fibrotic lesions showed larger absolute vascular measurements, fibrosis status was not independently associated with these parameters once lesion area was accounted for; thus, larger absolute values should not be interpreted as evidence of greater vascular network complexity. In contrast, baseline junction density—a measure of intra-lesional vascular connectivity—characterized the vision-improved subgroup and independently predicted short-term visual improvement. Preserved vascular connectivity, as reflected by higher junction density, may therefore denote a lesion phenotype more amenable to short-term visual recovery in fibrotic MNV, although the underlying biological mechanism remains to be elucidated.

Age also demonstrated an independent role in predicting visual improvement. Younger patients generally exhibit better capillary function and plasticity, with a greater capacity for microvascular network recovery following anti-VEGF therapy. This finding aligns with clinical observations, as increasing age is typically associated with retinal degenerative changes, vascular stiffening, and reduced MNV vascular remodeling capacity [23,24]. In the present study, the multivariable model incorporating age and junction density achieved an AUC of 0.77, suggesting acceptable predictive performance. Although an exploratory analysis based on a dichotomized junction density threshold yielded a higher AUC (0.87), this result was derived from data-driven categorization within the same cohort and requires external validation. These findings indicate that, in fibrotic MNV, vascular network integrity constitutes a fundamental factor, whereas age reflects overall microvascular health and reparative capacity, representing a potential clinical factor associated with visual recovery.

The main limitations of this study are its relatively small, single-center, retrospective design and the lack of ex-

ternal validation beyond bootstrap resampling, which limit generalizability of the findings. Second, we evaluated numerous OCT and OCTA parameters, creating a risk of false-positive associations due to multiple comparisons; the observed relationships should therefore be regarded as exploratory and require confirmation in larger prospective cohorts. Third, post-treatment assessment was performed after a single anti-VEGF injection rather than the standard three-dose loading phase. This reflects real-world PRN practice for established macular fibrosis but constrains inference regarding the full treatment response and long-term outcomes. Finally, and most importantly, our cohort included both treatment-naïve and previously treated patients (i.e., discontinued anti-VEGF therapy for ≥6 months), and prior treatment exposure was completely confounded with fibrosis status—all fibrotic eyes were previously treated, whereas all non-fibrotic eyes were treatment-naïve. As a result, the independent contributions of fibrosis and prior treatment could not be separated, and previous treatment represents a major potential confounder. Therefore, the observed differences between fibrotic and non-fibrotic lesions should not be interpreted as being attributable solely to fibrosis-related changes. Although the treatment-free interval was intended to mitigate the effects of recent therapy, persistent alterations in vascular architecture and fibrotic remodeling cannot be excluded, and incomplete historical treatment data precluded adjustment for cumulative treatment burden. Future prospective studies with standardized treatment histories and balanced inclusion of treatment-naïve and previously treated subgroups are warranted to clarify the independent impact of fibrosis on OCTA biomarkers and treatment outcomes. In addition, OCTA quantification required individualized adjustment of segmentation boundaries and image-processing parameters according to lesion characteristics. Although these procedures were performed following predefined criteria and by masked investigators, such manual adjustments and corrections may introduce measurement variability and potentially affect reproducibility across patients and imaging sessions. Future studies using standardized automated segmentation and analysis pipelines are warranted. Another limitation is the heterogeneity of anti-VEGF agents used within the fibrotic group. Although an exploratory subgroup analysis did not identify statistically significant differences in anatomical and visual outcomes between aflibercept- and IBI302-treated eyes, the two agents have distinct pharmacological mechanisms, with IBI302 additionally targeting complement components C3b/C4b. Given the relatively small sample size, the study may have been underpowered to detect potential differences related to treatment modality. Therefore, the potential influence of anti-VEGF agent heterogeneity on short-term treatment outcomes cannot be completely excluded. Future prospective studies with larger cohorts and standardized treatment regimens are warranted to further validate these findings.

In summary, our study highlights the potential clinical value of quantitative OCTA analysis in the management of fibrotic MNV. By assessing baseline junction density together with patient age at baseline evaluation, our findings suggest that these quantitative OCTA-derived parameters may provide potential prognostic information regarding short-term visual improvement after a single anti-VEGF therapy in fibrotic nAMD. The combination of vascular network characteristics and clinical factors may contribute to a better understanding of the heterogeneity of treatment outcomes in fibrotic lesions and may serve as a basis for the future development of predictive models.

Conclusion

Among fibrotic nAMD, baseline structural OCT characteristics were not significantly associated with short-term visual improvement, whereas OCTA revealed that MNV lesions observed in the fibrotic cohort had larger vessel area, greater total vessel length, more endpoints, greater central macular thickness, and worse baseline BCVA. However, these differences cannot be fully disentangled from the potential effects of prior treatment exposure, as fibrosis status was completely confounded with previous anti-VEGF treatment history in this cohort. Moreover, after adjustment for lesion area, the differences in absolute vascular parameters, including vessel area, total vessel length, and endpoint count, were no longer statistically significant, suggesting that these larger absolute vascular measurements may primarily reflect larger lesion size rather than increased intrinsic vascular complexity. Notably, higher baseline junction density and younger age emerged as independent predictors of visual improvement 4 weeks after a single anti-VEGF therapy in fibrotic MNV, and their combination demonstrated good predictive performance. These findings suggest that quantitative OCTA-derived vascular parameters may serve as potential indicators for characterizing fibrotic nAMD lesions and predicting short-term visual changes after a single anti-VEGF therapy.

Abbreviations

nAMD, neovascular age-related macular degeneration; VEGF, vascular endothelial growth factor; AUC, area under the curve; BCVA, best-corrected visual acuity; CFP, color fundus photography; CI, confidence interval; CMT, central macular thickness; ETDRS, Early Treatment Diabetic Retinopathy Study; IQR, interquartile range; IRF, intraretinal fluid; MCT, macular choroidal thickness; MF, macular fibrosis; MNV, macular neovascularization; OCT, optical coherence tomography; OCTA, optical coherence tomography angiography; OR, odds ratio; *p*, probability (*p* value); PRN, pro re nata; ROC, receiver operating characteristic; RPE, retinal pigment epithelium; SHRM, subretinal hyperreflective material; SPSS, Statistical Package

for the Social Sciences; SRF, subretinal fluid; SS-OCTA, swept-source optical coherence tomography angiography.

Availability of Data and Materials

The datasets generated and analysed during the current study are not publicly available due to patient confidentiality and institutional privacy policies, but are available from the corresponding authors on reasonable scientific request.

Author Contributions

XYZ and XCH contributed to drafting the manuscript, critically revising it for important intellectual content, and data acquisition. HXJ, YLQ, TS contributed to data acquisition and analysis and critically revised the manuscript. JQC and MWZ contributed to patient management, data acquisition, and data interpretation and critically revised the manuscript. YYG contributed to project administration, patient management, data acquisition, data interpretation and critically revised the manuscript. QYB contributed to the concept and design of the study, definition of intellectual content and critically revised the manuscript. YH contributed to the design of the study, critically revised the manuscript for important intellectual content, served as the guarantor of the study, and was responsible for funding acquisition. All authors gave final approval of the version to be published. All authors have participated sufficiently in the work to take public responsibility for appropriate portions of the content and agreed to be accountable for all aspects of the work in ensuring that questions related to its accuracy or integrity.

Ethics Approval and Consent to Participate

This study was conducted in accordance with the Declaration of Helsinki and was approved by the Medical Ethics Committee of Shanghai General Hospital (Approval number: [2026] 602). The requirement for written informed consent was waived by the ethics committee because of the retrospective nature of the study. All data were anonymized and de-identified prior to analysis.

Acknowledgment

We are grateful to the clinical and nursing staff at the Department of Ophthalmology, Shanghai General Hospital, for their assistance in patient recruitment and management. We also sincerely thank all the patients who volunteered to participate in this study.

Funding

This work was supported by grants from the National Natural Science Foundation of China (82301220, 82371025, 82388101, 82471077, 82571224), the National Key R&D Program (2023YFC2506100), the Basic-clinical collaborative project (JC202623), Shanghai Hospital Development Center Foundation (SHDC12024138), Shanghai Municipal Hospital Ophthalmology Specialist Alliance (SHDC22024304-A), and Science and Technology Commission of Shanghai Municipality (25ZR1401296).

Conflict of Interest

The authors declare no conflict of interest.

Supplementary Material

Supplementary material associated with this article can be found, in the online version, at https://doi.org/10.24976/Discov.Med.202638212.228.

References

[1] Xu H, Pu J, Yi C, Deng W, Yuan XL, Chen Z, et al. Macular fibrosis secondary to neovascular age-related macular degeneration: from clinic to biology. Progress in Retinal and Eye Research. 2026; 113: 101488. https://doi.org/10.1016/j.preteyeres.2026.101488

[2] Armendariz BG, Chakravarthy U. Fibrosis in age-related neovascular macular degeneration in the anti-VEGF era. Eye (London, England). 2024; 38: 3243–3251. https://doi.org/10.1038/s41433-024-03308-6

[3] Zhang J, Sheng X, Ding Q, Wang Y, Zhao J, Zhang J. Subretinal fibrosis secondary to neovascular age-related macular degeneration: mechanisms and potential therapeutic targets. Neural Regeneration Research. 2025; 20: 378–393. https://doi.org/10.4103/NRR.NRR-D-23-01642

[4] Bachmeier I, Armendariz BG, Yu S, Jäger RJ, Ebneter A, Glittenberg C, et al. Fibrosis in neovascular age-related macular degeneration: A review of definitions based on clinical imaging. Survey of Ophthalmology. 2023; 68: 835–848. https://doi.org/10.1016/j.survophthal.2023.03.004

[5] Romano F, Cozzi E, Airaldi M, Nassisi M, Viola F, Aretti A, et al. Ten-Year Incidence of Fibrosis and Risk Factors for Its Development in Neovascular Age-Related Macular Degeneration. American Journal of Ophthalmology. 2023; 252: 170–181. https://doi.org/10.1016/j.ajo.2023.03.033

[6] Hanson RLW, Airody A, Sivaprasad S, Gale RP. Optical coherence tomography imaging biomarkers associated with neovascular age-related macular degeneration: a systematic review. Eye (London, England). 2023; 37: 2438–2453. https://doi.org/10.1038/s41433-022-02360-4

[7] Nanji K, Grad J, Hatamnejad A, McKechnie T, Phillips M, Gemmy Cheung CM, et al. Baseline OCT Biomarkers Predicting Visual Outcomes in Neovascular Age-Related Macular Degeneration: A Meta-Analysis. Ophthalmology. 2025; 132: 1241–1252. https://doi.org/10.1016/j.ophtha.2025.06.018

[8] Zudaire E, Gambardella L, Kurcz C, Vermeren S. A computational tool for quantitative analysis of vascular networks. PloS One. 2011; 6: e27385. https://doi.org/10.1371/journal.pone.0027385

[9] Roberts PK, Nesper PL, Gill MK, Fawzi AA. SEMIAUTOMATED QUANTITATIVE APPROACH TO CHARACTERIZE TREATMENT RESPONSE IN NEOVASCULAR AGE-RELATED MACULAR DEGENERATION: A Real-World Study. Retina (Philadelphia, Pa.). 2017; 37: 1492–1498. https://doi.org/10.1097/IAE.0000000000001400

[10] Korobelnik JF, Chaudhary V, Mitchell P, Kang SW, Allmeier H, Lee J, et al. Aflibercept 2 mg for Neovascular Age-Related Macular Degeneration: XTEND at 3 Years. Ophthalmologica. Journal International D'ophtalmologie. International Journal of Ophthalmology. Zeitschrift Fur Augenheilkunde. 2025; 249: 17–29. https://doi.org/10.1159/000549663

[11] Rath S, Ibrahim AA, Singh A, Das A, Sediqi SM, Khan NA, et al. Efdamrofusp alfa: an insight into the novel drug and its use in age-related macular degeneration. International Journal of Retina and Vitreous. 2025; 11: 100. https://doi.org/10.1186/s40942-025-00685-2

[12] Toth LA, Stevenson M, Chakravarthy U. ANTI-VASCULAR ENDOTHELIAL GROWTH FACTOR THERAPY FOR NEOVASCULAR AGE-RELATED MACULAR DEGENERATION: Outcomes in Eyes With Poor Initial Vision. Retina (Philadelphia, Pa.). 2015; 35: 1957–1963. https://doi.org/10.1097/IAE.0000000000000583

[13] Souied EH, Addou-Regnard M, Ohayon A, Semoun O, Querques G, Blanco-Garavito R, et al. Spectral-Domain Optical Coherence Tomography Analysis of Fibrotic Lesions in Neovascular Age-Related Macular Degeneration. American Journal of Ophthalmology. 2020; 214: 151–171. https://doi.org/10.1016/j.ajo.2020.02.016

[14] Korva-Gurung I, Kubin AM, Ohtonen P, Hautala N. Visual Outcomes of Anti-VEGF Treatment on Neovascular Age-Related Macular Degeneration: A Real-World Population-Based Cohort Study. Pharmaceuticals (Basel, Switzerland). 2023; 16: 927. https://doi.org/10.3390/ph16070927

[15] Chang AA, Li H, Broadhead GK, Hong T, Schlub TE, Wijeyakumar W, et al. Intravitreal aflibercept for treatment-resistant neovascular age-related macular degeneration. Ophthalmology. 2014; 121: 188–192. https://doi.org/10.1016/j.ophtha.2013.08.035

[16] Amoaku WM, Chakravarthy U, Gale R, Gavin M, Ghanchi F, Gibson J, et al. Defining response to anti-VEGF therapies in neovascular AMD. Eye (London, England). 2015; 29: 721–731. https://doi.org/10.1038/eye.2015.48

[17] Bo Q, Yan Q, Shen M, Song M, Sun M, Yu Y, et al. Appearance of Polypoidal Lesions in Patients With Polypoidal Choroidal Vasculopathy Using Swept-Source Optical Coherence Tomographic Angiography. JAMA Ophthalmology. 2019; 137: 642–650. https://doi.org/10.1001/jamaophthalmol.2019.0449

[18] Nassisi M, Baghdasaryan E, Tepelus T, Asanad S, Borrelli E, Sadda SR. Topographic distribution of choriocapillaris flow deficits in healthy eyes. PloS One. 2018; 13: e0207638. https://doi.org/10.1371/journal.pone.0207638

[19] Schranz M, Told R, Hacker V, Reiter GS, Reumueller A, Vogl WD, et al. Correlation of vascular and fluid-related parameters in neovascular age-related macular degeneration using deep learning. Acta Ophthalmologica. 2023; 101: e95–e105. https://doi.org/10.1111/aos.15219

[20] Tenbrock L, Wolf J, Boneva S, Schlecht A, Agostini H, Wieghofer P, et al. Subretinal fibrosis in neovascular age-related macular degeneration: current concepts, therapeutic avenues, and future perspectives. Cell and Tissue Research. 2022; 387: 361–375. https://doi.org/10.1007/s00441-021-03514-8

[21] Roberts PK, Schranz M, Motschi A, Desissaire S, Hacker V, Pircher M, et al. Morphologic and Microvascular Differences Between Macular Neovascularization With and Without Subretinal Fibrosis. Translational Vision Science & Technology. 2021; 10: 1. https://doi.org/10.1167/tvst.10.14.1

[22] Faghihi S, Faghihi H, Bazvand F, Mehrabi Bahar M, Torkashvand A, Husein Ahmed A, et al. Baseline optical coherence tomography angiography biomarkers predict visual outcomes in treatment-naïve neovascular age-related macular degeneration patients. Scientific Reports. 2024; 14: 24528. https://doi.org/10.1038/s41598-024-75530-x

[23] Allaf AM, Wang J, Simms AG, Jiang H. Age-related alterations in retinal capillary function. Microvascular Research. 2023; 148: 104508. https://doi.org/10.1016/j.mvr.2023.104508

[24] Taylor TRP, Menten MJ, Rueckert D, Sivaprasad S, Lotery AJ. The role of the retinal vasculature in age-related macular degeneration: a spotlight on OCTA. Eye (London, England). 2024; 38: 442–449. https://doi.org/10.1038/s41433-023-02721-7